

evTransFER: A Transfer Learning Framework for Event-based Facial Expression Recognition

Rodrigo Verschae^{a,*}, Ignacio Bugueno-Cordova^a

^a*Institute of Engineering Sciences, Universidad de O'Higgins, Libertador Bernardo O'Higgins 611, Rancagua, O'Higgins, 2841959, Chile*

Abstract

Event-based cameras are bio-inspired sensors that asynchronously capture pixel intensity changes with microsecond latency, high temporal resolution, and high dynamic range, providing information on the spatiotemporal dynamics of a scene. We propose evTransFER, a transfer learning-based framework for facial expression recognition using event-based cameras. The main contribution is a feature extractor designed to encode facial spatiotemporal dynamics, built by training an adversarial generative method on facial reconstruction and transferring the encoder weights to the facial expression recognition system. We demonstrate that the proposed transfer learning method improves facial expression recognition compared to training a network from scratch. We propose an architecture that incorporates an LSTM to capture longer-term facial expression dynamics and introduces a new event-based representation called TIE. We evaluated the framework using both the synthetic event-based facial expression database e-CK+ and the real neuromorphic dataset NEFER. On e-CK+, evTransFER achieved a recognition rate of 93.6%, surpassing state-of-the-art methods. For NEFER, which comprises event sequence with real sensor noise and sparse activity, the proposed transfer learning strategy achieved an accuracy of up to 76.7%. In both datasets, the outcomes surpassed current methodologies and exceeded results when compared with models trained from scratch.

Keywords: Event-based Cameras, Transfer Learning, Deep Learning, Facial Expression Recognition, Facial Reconstruction

*Corresponding author
Email address: rodrigo@verschae.org (Rodrigo Verschae)

1. Introduction

Event-based neuromorphic vision sensors were introduced by [1], inspired by the asynchronous and sparse processing of biological vision systems. These event-based cameras are distinguished by their response to local intensity changes in a scene, generating an asynchronous event sequence that captures the timestamp and polarity associated with the brightness change of each pixel. Recent surveys on event-based cameras and their applications can be found in [2, 3, 4, 5].

Due to these novel vision sensors, many works have proposed event-data representations and methods targeted for this device(see e.g. [6, 7, 8]). This includes adapting traditional vision methods to event-based tasks, such as tracking [9, 10], image reconstruction [11, 12], and pattern recognition [13, 14]. Nevertheless, there is room for improvement in complex tasks, such as facial expression, where learning to handle short- and long-term spatiotemporal dynamics is essential. Moreover, few annotated datasets exist for event-based cameras; therefore, building accurate systems that do not rely on large, manually annotated datasets remains highly relevant.

To address these issues, we present evTransFER, a new learning framework for event-based facial expression recognition. This learning framework employs transfer learning to train an encoder that captures spatiotemporal dynamics in faces, incorporating a new event data representation to enhance recognition. To evaluate evTransFER, we use an event-based facial expression database called e-CK+ [15] and the NEFER dataset [16]. The proposed method outperforms current event-based methods on these datasets (one simulated and one real), particularly when compared with methods for similar problems. The project website, featuring additional information and materials, can be found at: <https://uoh-rislab.github.io/evtransfer>.

The remainder of this paper is organized as follows. Section 2 presents the state-of-the-art methods associated with event-based cameras and facial analysis. Section 3 describes representations, classification methods, available datasets, and tools for event-based cameras. Section 4 presents the proposed event-based facial expression recognition framework, evTransFER. Section 5 describes the experimental setup and Section 6

presents the evaluation results. Finally, Section 7 discusses these results, and Section 8 concludes and outlines future research.

2. Related Work

Face analysis is a well-studied area in computer vision, using classical and deep learning-based techniques to solve various problems [17, 18, 19]. For event-based facial analysis, several works report on neuromorphic face analysis [20], including face detection, eye blinking detection, and facial expression recognition, alongside tasks like (i) drowsiness-driving detection [21], (ii) isolated single-sound lip-reading [22], (iii) analyzing facial dynamics derived from speech [23], (iv) and understanding human reactions [24]. The following discussion reviews research on the problems of face detection, eye tracking, blinking, and facial expression recognition.

Face Detection. [25] introduces a patch-based model for face detection, highlighting the potential of these sensors for low-power vision applications. [26] exploited event temporal resolution properties to detect faces using eye blinks (characterized by unique temporal signatures) and applied a probabilistic framework for face localization and tracking in indoor and outdoor environments. Ramesh et al. [27] presented an event-based method for learning face representations using kernelised correlation filters within a boosting framework for surveillance applications. In [28], the authors introduced the Faces in Event Streams (FES) dataset, providing 689 minutes of annotated event camera data for event-based face detection. To demonstrate its effectiveness, they trained 12 models to predict bounding box and facial landmark coordinates, achieving real-time detection with an mAP50 score of over 90%. In [29], the authors presented a multispectral event-based vision system for face detection (*MS-EVS*). They introduced three neuromorphic datasets (N-MobiFace, N-YoutubeFaces, and N-SpectralFace), combining RGB videos with simulated color events and multispectral videos. The authors showed that early fusion of multispectral events improved face detection performance over conventional multispectral images, demonstrating the value of multispectral event data.

Eye Blinking/Tracking. In [26], the authors used blinks to track errors in faces through a generic temporal model correlated with local face activity. [30] proposed a hybrid event-based near-eye gaze tracking system with update rates beyond 10,000 Hz, integrating an online 2D pupil fitting method that updates a parametric model using a polynomial regressor to estimate the gaze point. [31] proposed BRAT, an event-based eye-tracking method combining CNN features with Bi-GRU and attention, achieving state-of-the-art accuracy on ThreeET-plus. [32] introduced TDTracker, which uses 3D CNNs and GRU-based modules to capture temporal dynamics and ranked third in the CVPR 2025 challenge. [33] presented KnightPupil, integrating EfficientNet-B3, bidirectional GRU, and a state-space module to enhance robustness against abrupt eye movements, with competitive results on 3ET+.

Facial Expression Recognition. In [34], the authors presented *Spiking-FER*, a Spiking Neural Network (SNN) for facial expression recognition. The original datasets were downsampled to 200×200 pixels and converted to event sequences using neuromorphic emulation tools. Results show the SNN achieves performance comparable to conventional deep neural networks while reducing energy consumption (up to 65.39 times). The NEFER dataset [16] combines RGB videos and events for emotion recognition, capturing micro-expressions difficult to detect with RGB data but evident in event data. Results show that the event-based approach doubles accuracy compared with RGB-based methods, demonstrating neuromorphic effectiveness in analyzing fast expressions. [15] presents an analysis of event-based gesture and facial expression recognition. Deep Learning-based classification models were evaluated across various settings using gesture-recognition databases and two synthetic facial-expression databases (e-MMI and e-CK+).

3. Preliminaries

This section provides an overview of event-based cameras and synthesizes research on data representations, classification methods, neuromorphic datasets, and tools for event-based data generation, including simulators and emulators. This description is required to introduce the proposed method and its evaluation.

Most studies that have addressed classification problems of event data have used a process similar to that shown in Figure 1. This process involves an event representation that captures spatial and temporal progression, a feature extractor, a classification layer, and sometimes a sequence module for analyzing temporal patterns.

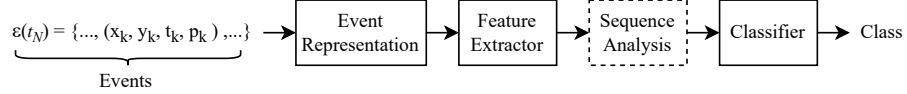


Figure 1: Pipeline for event-based classification that addresses the need of (i) a representation that captures the event’s spatial distribution and asynchronous temporal evolution, (ii) a feature extractor that properly encodes the input information, (iii) an analysis over a long sequence of events, (iv) a classifier module.

3.1. Event generation model

Event cameras are sensors where each pixel independently responds to changes in the received logarithmic brightness signal $L(\mathbf{u}_k, t_k) \doteq \log(I(\mathbf{u}_k, t_k))$, where \mathbf{u}_k is the sensor pixel, t_k is the associated time, I is the brightness signal, and L is the log-brightness [2]. An event is triggered at pixel $\mathbf{u}_k = (x_k, y_k)^T$ and time t_k when the brightness change since the last event reaches a threshold $\pm C > 0$:

$$L(\mathbf{u}_k, t_k) - L(\mathbf{u}_k, t_k - \Delta t_k) = p_k C, \quad (1)$$

where $p_k \in \{-1, +1\}$ is the brightness change sign, and Δt_k is the time since the last event at \mathbf{u}_k . In a time interval, an event camera produces a sequence $\mathcal{E}(t_N) = \{e_k\}_{k=1}^N = \{(\mathbf{u}_k, t_k, p_k)\}_{k=1}^N$, where t_N denotes the last timestamp in sequence \mathcal{E} .

3.2. Event representations

A critical issue is extracting meaningful information from event sequences. The basic level of representation is an individual event, consisting of coordinates, timing, and polarity. A second level is an event packet, which corresponds to a spatiotemporal neighborhood of events. Some representations accumulate events in the image plane. Other representations are obtained by preprocessing events into dense images or tensors for image-based models, which are then used in convolutional neural networks.

Some prior representations include [2]: a) Event frame or 2D histogram, b) Time surface: 2D map where pixels store a time value, c) Voxel Grid: space-time 3D histogram of events, where voxels represent pixels and time intervals, d) 3D point set: events in the spatio-temporal neighborhood processed as points in 3D space, e) Point sets on image plane: Events as evolving 2D points on image plane, f) Motion-compensated image: representation based on events and motion hypothesis, and g) Reconstructed images: a more motion-invariant representation of event frames.

These representations do not fully leverage the rich spatiotemporal information of event sequences and hinder fast processing by requiring the integration of information across time. Thus, another approach uses representations that characterize the spatiotemporal distribution of events, such as the Event Spike Tensor [6], Sparse Recursive Representation [35], Temporal Binary Representation [8, 36], Time-Ordered Recent Event Volumes [37], Neighborhood Suppression Time Surface [38], Binary Event History Image [39], and Tencode [40]. In the following section, we describe SSR and EST, two relevant representations considered later in this article.

Sparse Recursive Representations (SSR). In [35], the authors proposed an image-like representation $H_{t_N}(\mathbf{u}, c)$ for an event sequence $\mathcal{E}(t_N)$, where $\mathbf{u} = (x, y)^T$ denotes a pixel, and c denotes a channel. This representation can be processed by standard CNNs and preserves the spatial sparsity of events, but discards the temporal sparsity. The authors propose to recover the temporal sparsity by focusing on the change in $H_{t_N}(\mathbf{u}, c)$ when a new event arrives:

$$H_{t_{N+1}}(\mathbf{u}, c) = H_{t_N}(\mathbf{u}, c) + \sum_i \Delta_i(c) \delta(\mathbf{u} - \mathbf{u}'_i), \quad (2)$$

leading to increments $\Delta_i(c)$ at only a few positions \mathbf{u}'_i in $H_{t_N}(\mathbf{u}, c)$, to maximize efficiency, and using Dirac pulses $\delta(\mathbf{u} - \mathbf{u}'_i)$.

The Event Spike Tensor (EST). In [6], the authors converted the event set $\mathcal{E}(t_N)$ into a grid-based representation, preserving spatial, temporal, and polarity information. To use this in standard deep learning networks (e.g., CNNs), it is necessary to map sequence \mathcal{E} to tensor \mathcal{T} , that is, $\mathcal{M} : \mathcal{E} \rightarrow \mathcal{T}$.

Given that events represent point sets in a four-dimensional manifold spanned by the x and y spatial coordinates, time, and polarity, [6] proposes a grid representation:

$$S_{\pm}[x_l, y_m, t_n] = \sum_{e_k \in \mathcal{E}_{\pm}} f_{\pm}(x_k, y_k, t_k) h(x_l - x_k, y_m - y_k, t_n - t_k), \quad (3)$$

where f_{\pm} is an event Measurement Field (e.g., encoding temporal or polarity information) and h is an aggregation kernel.

Typically, the spatiotemporal coordinates, x_l, y_m, t_n , lie on a voxel grid, that is, $x_l \in \{0, 1, \dots, W - 1\}$, $y_m \in \{0, 1, \dots, H - 1\}$, and $t_n \in \{t_0, t_0 + T, \dots, t_0 + BT\}$, where t_0 is the first timestamp, T is the bin size, and B is the number of temporal bins.

3.3. Event-based classification methods

Several models have been designed to capture the temporal evolution of events, including SNNs, graph-based convolutional networks [41] and asynchronous event processing [35]. In this subsection, we examine two learning models associated with the previously reviewed representations [6, 35] and summarize the other relevant classification models.

For end-to-end representation learning of asynchronous event-based data, in [6] EST feeds a CNN with ResNet-34 as backbone. It uses a fully connected layer to detect processed features and a softmax activation function to assign a probabilistic distribution to each class. This architecture has been used for object recognition (e.g. in the N-Caltech101 dataset [42]) and gesture recognition (e.g. the DVS128 Gesture Dataset [43]). In [15], the method achieved 93.82% accuracy in event-based gesture recognition.

A second method is Asynchronous Sparse Convolutional Networks (Asynet) [35], in which a sparse representation of events and a Sub-manifold Sparse Convolutional (SSC) network are learned. This method exploits spatio-temporal sparsity in classical convolutional architectures by reducing computational power and processing events asynchronously. The authors described two variants: *Dense* and *Sparse*. Both variants process sparse representations asynchronously but differ in that the first uses a traditional CNN, whereas the second uses the SSC network. [15] reports that on the

DVS128 Gestures dataset, the Asynet architecture outperforms end-to-end representational learning method [6] in gesture recognition, achieving 94.66% accuracy versus 93.82%. According to the authors, this is mainly due to the SSR and SSC networks for asynchronous events; however, this method has high inference time.

Studies on event-based cameras have explored approaches for designing novel spatio-temporal learning models. [44, 45, 46] employed SNNs in classification tasks to exploit the spatio-temporal distribution of events, responding to signals exceeding activation thresholds. [47, 48] used traditional classification models, such as SVMs, and benefited from adaptive kernels that capture temporal data evolution. [49] adopted a CNN-based architecture coupled with an LSTM layer to capture events' spatial and temporal distribution. [50] incorporated a Deep Recurrent Neural Network for human activity recognition, where the network becomes deep in time and spatial domains.

3.4. Datasets and data generation using simulators/emulators of event-based cameras

A key challenge in exploring new supervised learning tasks is the availability of databases. For event-based facial analysis, databases are limited, including: for face detection are Face Detection dataset [26], N-MobiFace [29], N-YoutubeFaces [29], and N-SpectralFace [29], while the DAVIS-Face dataset [27] and Neuromorphic-Helen dataset [51] are available for eye tracking and blink recognition. For face expression recognition, recent datasets include NEFER [16], DVS-CK+ [34], DVS-ADFES [34], DVS-CASIA [34], DVS-MMI [34], e-CK+ [15] and e-MMI [15].

Given the lack of data on many problems involving event-based cameras, some datasets have been generated using simulators/emulators, such as N-MobiFace, N-YoutubeFaces, e-CK+, and e-MMI. Two methods for generating realistic events from video frames are ESIM [52] and V2E [53]. ESIM simulates an event camera using an adaptive rendering scheme that samples frames as needed [52]. The V2E simulator aims to replicate event cameras by generating realistic DVS event sequences with high temporal resolution (using an interpolation model [54]), high dynamic range (by computing the luminance intensity logarithm), pixel-level Gaussian event-threshold mismatch, a finite intensity-dependent bandwidth, and intensity-dependent noise [53]. In [15] the e-CK+ dataset was introduced, in which emulated events were generated from

frames using V2E, and an event-frame pair was available for each sample.

4. evTransFER: a framework for event-based facial expression recognition

The present section describes the proposed learning framework, evTransFER. This framework addresses: a) the design of a representation that considers the temporal distribution of events, b) the use of an encoder as a feature extractor obtained by transfer learning (to have prior knowledge of the task), and c) the integration of a spatio-temporal sequential module, and it is based on the architecture shown in Figure 2. The modules and training methodologies of the proposed architecture are described in the following sections.

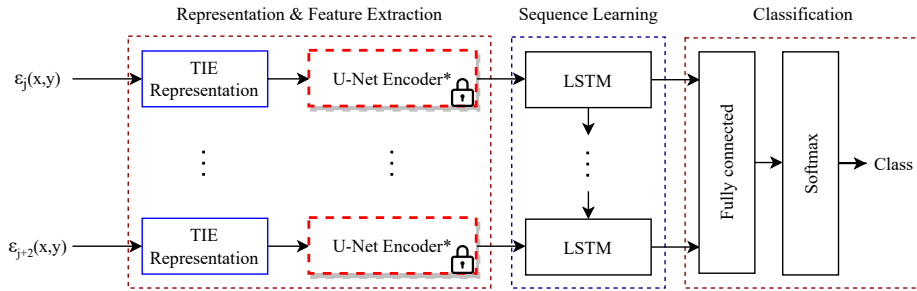


Figure 2: Proposed Architecture for event-based facial expression recognition, comprising (i) a new event representation called TIE (Temporal Information of Events), (ii) a feature extractor module for identifying and encoding events’ key patterns (encoder trained for face reconstruction, see Section 4.2), (iii) temporal memory networks enabling temporal learning of event sequences, and (iv) a classification module that categorizes events into facial expressions.

4.1. Proposed Temporal Information of Events (TIE) representation

We begin by outlining the proposed Temporal Information of Events (TIE) representation, which is grounded in the Event Spike Tensor [6] mentioned earlier.

Temporal encoding. As outlined in Section 3.2, EST is a representation that captures spatio-temporal information of events within a voxel grid data structure. The analytical expression of the voxel grid corresponds to sampling the convolved signal at regular intervals (see Equation 3). A challenge with this representation stems from temporal coding and lack of timestamp normalization in the event sequence, which affects the

measure function $f_{\pm}(x_k, y_k, t_k)$ and kernel $h(x_l - x_k, y_m - y_k, t_n - t_k)$. We observe that temporal encoding and normalization methods significantly influence classification accuracy. To address this, we define the temporal variables as $\tau_k = \frac{t_k}{t_N}$, $\hat{\tau}_k = \frac{t_k - t_1}{t_N - t_1}$ and establish two measure functions based on τ_k and $\hat{\tau}_k$:

$$\begin{aligned} f_{\tau_k} &= f_{\pm}(x_k, y_k, \tau_k) = \tau_k = \frac{t_k}{t_N}, \\ f_{\hat{\tau}_k} &= f_{\pm}(x_k, y_k, \hat{\tau}_k) = \hat{\tau}_k = \frac{t_k - t_1}{t_N - t_1}, \end{aligned} \quad (4)$$

then the kernel can be evaluated in τ_k and $\hat{\tau}_k$ (see Equation 4):

$$h_{\tau_k} = h(x_l - x_k, y_m - y_k, \tau_n - \tau_k), \quad (5)$$

$$h_{\hat{\tau}_k} = h(x_l - x_k, y_m - y_k, \hat{\tau}_n - \hat{\tau}_k), \quad (6)$$

with $\tau_n - \tau_k = \frac{t_n - t_k}{t_N}$ and $\hat{\tau}_n - \hat{\tau}_k = \frac{t_n - t_k}{t_N - t_1}$.

Tensor mapping. The EST representation converts event sequences into grid-based structures, effectively preserving spatial, temporal, and polarity information. Due to the dimensional complexity inherent in this structure, we project this representation into images, thereby enabling the utilization of existing deep learning-based architectures designed for three-channel inputs.. To achieve this, we first take the EST and reshape it starting from the tensor $S \in \mathbb{R}^{(C,H,W)}$ to a tensor $\hat{S} \in \mathbb{R}^{(C, \frac{2C}{3}, H, W)}$:

$$S = \left(S_k^{i,j} \right)_{1 \leq k \leq C}^{1 \leq i \leq W, 1 \leq j \leq H}, \hat{S} = \left(\hat{S}_{k,l}^{i,j} \right)_{1 \leq k \leq C, 1 \leq l \leq \frac{2C}{3}}^{1 \leq i \leq W, 1 \leq j \leq H}, \quad (7)$$

with C the number of input channels (e.g. $C = 9$), H, W the height and the width of the representation, respectively, k the channel index, i the horizontal index, j the vertical index, and l the bin index. Then, the values of the \hat{S} bin, grouped along the time axis, are then summed up into a tensor $\hat{Z} \in \mathbb{R}^{(3,H,W)}$, which is subsequently normalized:

$$\hat{Z} = \left(\hat{Z}_k^{i,j} \right)_{1 \leq k \leq 3}^{1 \leq i \leq W, 1 \leq j \leq H}, \quad \hat{Z}' = \frac{\hat{Z} - \hat{Z}_m}{\hat{Z}_M - \hat{Z}_m}, \quad (8)$$

where \hat{Z}_m and \hat{Z}_M are the 1% and 99% percentiles of \hat{Z} .

Finally, \hat{Z}' is mapped from $[0, 1] \rightarrow [0, 255]$ (saturating values outside the 1% and 99% percentiles), to generate the projection in the RGB image space. We refer to our proposed event-based data representation as *Temporal Information of Events* (TIE). Figure 3 illustrates the process to obtain the TIE representation.

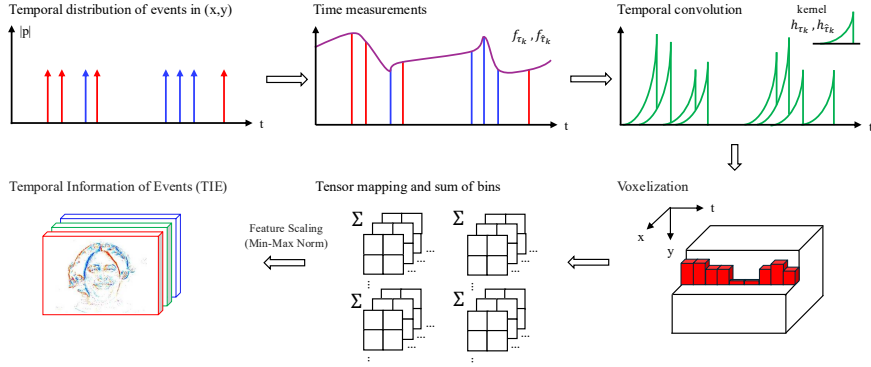


Figure 3: Pipeline of the proposed representation: *Temporal Information of Events* (TIE). TIE is based on the EST representation [6].

We recall that τ is a temporal variable that characterizes the distribution of events. In the experiments detailed in Section 6, we assess four TIE variants ($f_{\tau_k} \cdot h_{\tau_k}$, $f_{\tau_k} \cdot h_{\hat{\tau}_k}$, $f_{\hat{\tau}_k} \cdot h_{\tau_k}$, and $f_{\hat{\tau}_k} \cdot h_{\hat{\tau}_k}$), taking into account different normalization factors and kernels. Figure 4 illustrates an example of how these variants are used.

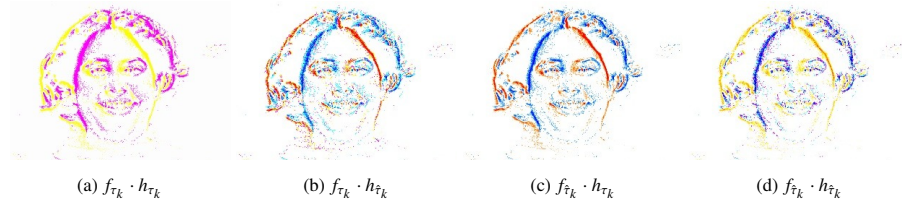


Figure 4: Variants of TIE event representation generated from the e-CK+ dataset by changing the temporal variable $\tau \in \{\tau_k, \hat{\tau}_k\}$, parameter of measurement function f and the kernel function h .

4.2. Feature extractor training for knowledge transfer

A crucial element of a feature-rich extractor network is the accurate characterization and encoding of the input information for the learning model. For complex tasks, the network should possess prior knowledge to effectively identify relevant patterns.

We propose using event-based facial reconstruction to acquire prior knowledge about face spatio-temporal dynamics, which can then be utilized (as an encoder) in facial expression recognition. For this approach, we only need samples of event sequences and their corresponding image frames, without requiring additional annotations. This methodology can be readily applied to other problems. This event-based pipeline can be trained using asynchronous events and synchronous frames from a DAVIS346 camera, simulated events from videos, or co-axial imaging setups (which include a beam splitter, an event camera, and an RGB camera, such as the one used in [55]). Then the obtained encoder can provide prior knowledge.

Learning from prior knowledge. The process of reconstructing image frames involves acquiring representations that capture the structural and dynamic characteristics. For facial expressions, this process involves developing a feature extractor by reconstructing facial images. This approach assumes that spatiotemporal dynamics in reconstructed faces are valuable for accurate expression classification. Our proposal follows these ideas and incorporates the *pix2pix* [56] generator encoder for feature extraction. We employ a U-Net-based encoder-decoder [57] trained using a conditional Generative Adversarial Network (cGAN) for image reconstruction tasks. This framework uses the TIE representation as a latent variable, with the original frame as the expected output. The cGAN architecture has two networks: a generator that takes a latent variable to replicate a distribution, and a discriminator that distinguishes real samples from generated ones. The architecture in Figure 5 serves as an event-based reconstruction network. Subsequently, we use the encoder as a feature extractor for the facial expression classifier.

In the cGAN, the generator G seeks to minimize the difference in the reconstruction of facial expressions from events, while the discriminator D seeks to maximize it. The optimization problem to be solved is $\min_G \max_D \mathbb{L}_{cGAN}(G, D)$, with:

$$\begin{aligned} \mathbb{L}_{cGAN}(G, D) = & \mathbb{E}_{f_{real}, f_{gen}} [\log(D(f_{real}, f_{gen}))] \\ & + \mathbb{E}_{e_{TIE}} [\log(1 - D(f_{real}, G(e_{TIE})))] \end{aligned} \quad (9)$$

where \mathbb{L}_{cGAN} is the loss function, \mathbb{E} the expected value, f_{real} the images frames, e_{TIE}

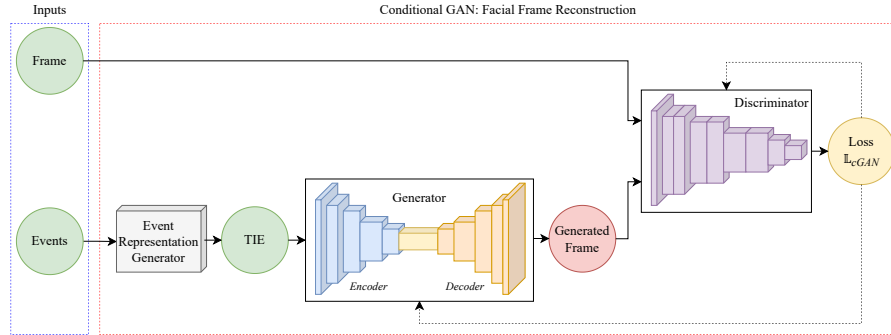


Figure 5: Proposed architecture for event-based facial frame reconstruction. The architecture involves a conditional Generative Adversarial Network that reconstructs frames from a latent variable. This reconstruction system comprises three components: (i) the TIE representation, which serves as a latent variable; (ii) the generator network, which is responsible for reconstructing facial frames from events; and (iii) the discriminator network, which assesses the likelihood of the generated frame against the original frame, providing feedback to the generator based on the loss incurred. The system accepts two inputs: an event sequence and the corresponding frames.

the TIE event-based data representation as latent variable, and f_{gen} the generated face frame from the generator autoencoder. By addressing the min-max loss problem, as shown in Figure 6, we obtain an encoder that uses the TIE representation to reconstruct a facial frame. Once trained for face reconstruction, the encoder is integrated into the proposed facial expression recognition system, as explained in the next section.

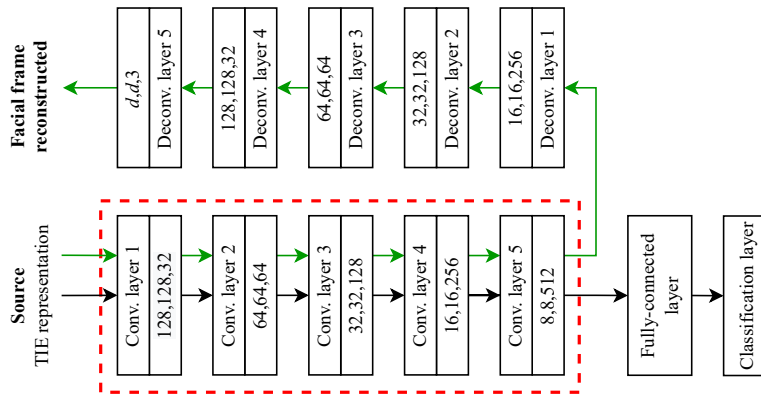


Figure 6: Architecture for training CNN feature extractor in event-based facial frame reconstruction, where prior knowledge and learning transfer for event-based facial expression recognition. The obtained encoder (transferred weights) is shown in red dashed lines, and the reconstruction cycle in green lines. d, d corresponds to the spatial dimension of the reconstructed frame.

4.3. Proposed Architecture

Now we describe in detail the proposed architecture, already shown in Figure 2. The proposed system receives an \mathcal{E}_j event sub-sequence as input. Following the Stacking Based on Time approach by [11], the events in-between the time references of two consecutive intensity images of the event camera (denoted as Δt) are sequenced in $\mathcal{E}_j(x, y)$. Here, the time duration of the event sequence is divided into n equal-scale portions, and then $\mathcal{E}_j(x, y)$ is built by sequencing the events in each time interval $\left[\frac{(j-1)\Delta t}{n}, \frac{j\Delta t}{n}\right]$. Thus, each $\mathcal{E}_j(x, y)$ sub-sequence is generated from time windows, that is, $\mathcal{E}_j(x, y) = f(j, \Delta t)$, where f is a function that converts event sequences into samples with fixed time windows. Subsequently, the TIE representation is produced for each event sub-sequence, encoding its spatiotemporal distribution. This representation feeds the U-Net Encoder with static weights (acting as a feature extractor) to learn the temporal sequence of events using an LSTM. Finally, the classification module uses a Sequence Learning module (LSTMs) connected via a fully connected layer to a softmax to characterize and correlate the sequence of events, thereby classifying the sequence into their respective facial expressions.

With this, we implement a transfer learning from face frame reconstruction to the U-Net encoder. The proposed training procedure, in addition to transferring the trained encoder weights (from the U-Net architecture), fine-tunes all network weights.

In summary, the proposed architecture comprises three key components: the event representation module, feature extractor module, and sequence learning module, implemented using the previously described TIE representation, U-Net-based Encoder, and three LSTM units, respectively.

5. Experimental Setup

The current section details the experimental setup for training and evaluating the proposed framework, encompassing a) the two datasets utilized, b) the training parameters for encoder learning, and c) the training parameters for the evaluated state-of-the-art methods. In Section 6, we compare our approach with state-of-the-art methods and conduct an ablation study on it. Section 7 discusses the results obtained.

5.1. Datasets

5.1.1. The Event CK+ dataset

The *Cohn-Kanade Extended (CK+)* dataset [58] is among the most frequently used frame-based benchmark datasets for facial expression recognition. Initially, the Cohn-Kanade dataset [59] was created for Action Unit and Valence-Arousal recognition; however, the authors subsequently expanded it to include facial expression analysis.

CK+ comprises 593 video sequences featuring 123 subjects aged 18-50, representing diverse genders and heritages. Each video corresponds to a facial transition from a neutral expression to a specific peak expression, recorded at 30 frames per second (FPS) with a resolution of either 640x490 or 640x480 pixels. Among these videos, 327 were categorized under one of the following seven expressions: anger, contempt, disgust, fear, happiness, sadness, and surprise (examples are provided in Figure 7).

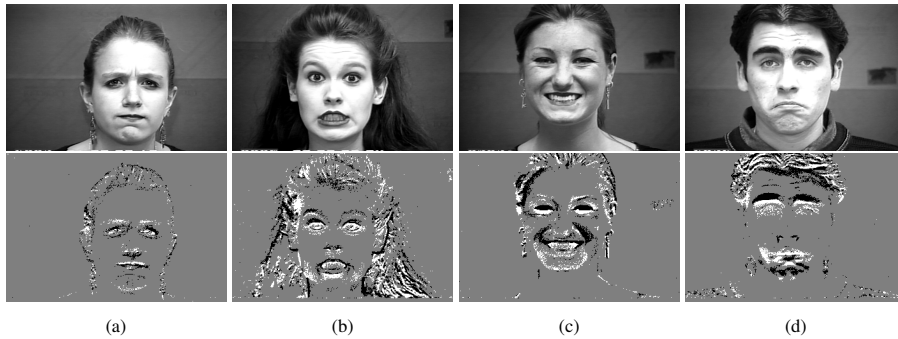


Figure 7: The Event-based Extended Cohn-Kanade Dataset (e-CK+) [15]: A event-based dataset for individual facial expression recognition. Examples from the e-CK+ dataset[59, 58]: (a) Anger, (b) Fear, (c) Happiness, (d) Sadness. Top: original image. Bottom: Accumulated event representation visualization, where white and black pixels correspond to events with positive and negative polarity, respectively.

Due to the frame-based nature of the image sequences of CK+, we follow [15] and use the e-CK+ dataset, an event-based equivalent of CK+ generated via the V2E emulation method [53], which produces event sequences with high temporal resolution and dynamic range. Table 1 shows the parameters of V2E used to elaborate the database. We build the e-CK+ for a 346x260 (frames and events), emulating the sensor resolution of the DAVIS346 camera. Before emulating the events, data augmentation of the CK+ database samples was performed, including horizontal flipping and four random

rotations (ranging from -10° to 10°). Additionally, the frames in this dataset are not landmark-standardized.

Table 1: Parameters used to generate the e-CK+ database [15]. This dataset is used to train and validate the event-based facial expression recognition methods.

Input data	Frames with 640x480 pixels
DVS timestamp resolution	1 ms
DVS exposure duration	5 ms
Positive/Negative event threshold	0.15
Sigma threshold variation	0.03
Emulated event camera device	DAVIS346
Output Spatial dimensions	346x260
Cut-off frequency	30 Hz
Output data	Frames/events

Therefore, after the event sequence for the 327 CK+ videos was synthetically generated, the class samples were split into training and validation datasets in an 80%-20% ratio. Now, following the procedure described in Section 4.3, a time window $\Delta t = 30\text{fps}$ ($\sim 33\text{ms}$) is used to generate the e-CK+ samples for this work (based on the CK+ fps) and match the events sub-samples with the respective original frames. Example results are shown in Figure 7, bottom row. Finally, the frames and event representations were spatially cropped at a 1:1 ratio for frame reconstruction and facial expression classification.

5.1.2. The NEFER dataset

NEFER [16] is a real-world event-based facial expression database offering three synchronized modalities for each sample: (i) RGB frames captured with a GoPro camera at 60 fps, (ii) event-derived frame representations calculated with a temporal binning of 15 ms, and (iii) the original raw event sequence in .raw format recorded using a Prophesee sensor. These modalities enable direct temporal correspondence between frame-based and event-based signals.

This dataset focuses on facial expression and emotion analysis and includes sequences of both spontaneous and posed expressions under varying head poses and illumination conditions. Crucially, the dataset includes only expression annotations and lacks both bounding boxes and facial landmarks. To address this issue, we cropped the face and event regions using the following procedure: to achieve consistent spa-

tial localization across both modalities, we employed a two-stage process: first, we detected faces in RGB frames using a face detector; subsequently, we approximated facial locations in the event domain through DBSCAN-based clustering on event coordinates, followed by manual refinement. With these aligned detections, we estimated the geometric transformation between frames and events and utilized this mapping to generate bounding boxes for the remaining RGB frames, event TIE frames, and raw event windows.

One practical challenge of NEFER is that many samples exhibit very low event activity, such as near-static facial motion. Consequently, we excluded frame-event pairs whose event windows failed to meet a minimal activity threshold, ensuring that the evaluation of evTransFER was based on samples with significant spatiotemporal content. Due to data protection restrictions, we do not reproduce visual examples from NEFER; readers are directed to [16] for illustrations and further details about the dataset.

5.2. Learned encoder from face image reconstruction

As described in Section 4.2, we trained the face reconstruction system and extracted its encoder using paired frame–event data from both the e-CK+ and NEFER datasets. For e-CK+, the reconstruction network was trained on the emulated event sequence and the corresponding CK+ frames. For NEFER, raw event sequences were aligned with the GoPro RGB frames provided by the dataset (only the detected face regions were used). This training setup allows the encoder to learn spatiotemporal facial dynamics from both synthetic and real neuromorphic data.

Table 2 summarizes the architecture and training parameters of the event-based facial frame reconstruction model. The system is trained for 100 epochs using the Adam optimizer with a learning rate of 0.0002 and a binary cross-entropy loss.

5.3. Training of the event-based facial expression recognition methods

Table 3 summarizes the hyperparameters employed in training of evTransFER, as well as the ones of the state-of-the-art methods used in the evaluations in Section 6.

Table 2: Architectures and training parameters of the event-based facial frame reconstruction method.

Parameter	Generator	Discriminator
Architecture	U-Net	PatchGAN
Weight Initialization	$\mathcal{N}(\vec{w} \mu = 0, \sigma^2 = 0.02^2)$	$\mathcal{N}(\vec{w} \mu = 0, \sigma^2 = 0.02^2)$
Batch Normalization	Yes	Yes
Dropout	Encoder: No	No
	Decoder: Yes, 0.5 dropout	
Activation Function (Interm. Layers)	Encoder: LeakyReLU ($\alpha=0.2$)	LeakyReLU ($\alpha=0.2$)
	Decoder: ReLU	
Activation Function (Last Layer)	Tanh	Sigmoid

Table 3: Training parameters used for event-based facial expression recognition methods. evTransFER: U-Net trained for Face Reconstruction and later Fine-Tuned.

Parameter	EST + CNN [6]	Asynet CNN / SSC [35]	ViT [60]	evTransFER*
Backbone	ResNet-34	VGG-16	VIT B16	U-Net Encoder
Epochs / Batch Size	30 / 4	30 / 32	20/4	30 / 32
Learning Rate (Adam)	0.0001			
Learning Rate Sched.	ExponentialLR	ExponentialLR	None	ExponentialLR
γ (LR Scheduler)	0.5	0.1	None	0.1
Loss Function	Cross Entropy			

6. Evaluation

In the present Section, a comparative evaluation of the event-based facial expression recognition is performed, including: i) an evaluation of the performance effects of TIE variants and the use of LSTM (Section 6.2), ii) a comparative analysis of the proposed method and state-of-the-art methods (Section 6.3), and iii) an ablation study that shows the contribution of the different techniques used in the proposed classification architecture is performed (Section 6.4).

6.1. TIE representation and Event-based facial frame reconstruction

To assess the quality of the learned encoder prior to its transfer to the facial expression recognition task, we evaluate the event-based facial frame reconstruction performance on both the e-CK+ and NEFER datasets.

The reconstruction network is trained using paired event representations and RGB frames, and the encoder extracted from this model is later reused as the feature extractor in evTransFER. Table 4 and Table 5 report quantitative results at epoch 80 for the four temporal-domain and kernel combinations described in Section 4. Figure 8 provides qualitative examples of the e-CK+ generated frames.

Table 4: Event-based facial reconstruction performance on the **e-CK+** dataset at epoch 80, comparing temporal-domain and kernel-based combinations. The best values for each metric are shown in bold.

Metric	e-CK+ Facial Reconstruction Results			
	$f_{\tau_k} \cdot h_{\tau_k}$	$f_{\hat{\tau}_k} \cdot h_{\hat{\tau}_k}$	$\hat{f}_{\tau_k} \cdot h_{\tau_k}$	$\hat{f}_{\hat{\tau}_k} \cdot h_{\hat{\tau}_k}$
MSE	0.0017	0.0010	0.0015	0.0020
RMSE	0.0403	0.0319	0.0388	0.0446
MAE	0.0271	0.0210	0.0266	0.0301
PSNR	27.9830	30.0284	28.3061	27.1474
SSIM	0.8477	0.8826	0.8640	0.8188
NCC	0.9897	0.9927	0.9903	0.9869

As shown in Table 4, the $f_{\tau_k} \cdot h_{\hat{\tau}_k}$ representation consistently yields the best e-CK+ facial reconstruction quality across all metrics (MSE, RMSE, MAE, PSNR, SSIM, and NCC). This indicates that normalizing timestamps with respect to the global event window ($\hat{\tau}_k$) while filtering with a kernel defined in the absolute temporal domain (h_{τ_k}) provides the most stable temporal encoding for emulated event data. Qualitative results in Figure 8 confirm that this representation preserves facial structure more accurately and reduces temporal noise introduced by rapidly changing event rates.

A similar performance is observed for NEFER (Table 5), despite the increased difficulty of reconstructing from raw, real event sequence. Again, $f_{\tau_k} \cdot h_{\hat{\tau}_k}$ achieves the strongest performance across all metrics, with clear improvements over other variants. Real event data naturally exhibit greater sparsity, device noise, and nonlinear motion dynamics, which explains lower absolute PSNR and SSIM values than e-CK+. Nevertheless, the results demonstrate that the temporal normalization used in $h_{\hat{\tau}_k}$ effectively compensates for non-uniform event rates and exposure differences present in real neuromorphic samples.

Table 5: Event-based facial reconstruction performance on the **NEFER** dataset at epoch 80, comparing temporal-domain and kernel-based combinations. The best values for each metric are shown in bold.

Metric	NEFER Facial Reconstruction Results			
	$f_{\tau_k} \cdot h_{\tau_k}$	$f_{\hat{\tau}_k} \cdot h_{\hat{\tau}_k}$	$\hat{f}_{\tau_k} \cdot h_{\tau_k}$	$\hat{f}_{\hat{\tau}_k} \cdot h_{\hat{\tau}_k}$
MSE	0.0030	0.0019	0.0025	0.0055
RMSE	0.0541	0.0440	0.0495	0.0715
MAE	0.0389	0.0297	0.0326	0.0532
PSNR	25.4543	27.2208	26.2032	23.2468
SSIM	0.8127	0.8358	0.8226	0.7564
NCC	0.9851	0.9867	0.9833	0.9755

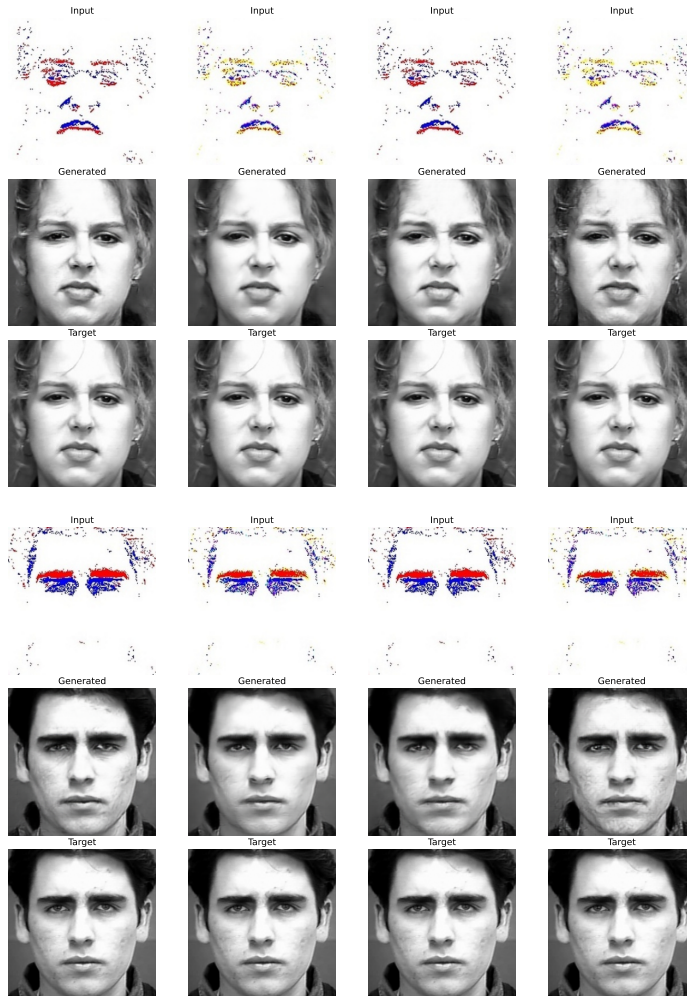


Figure 8: Event-based facial frame reconstruction results after 80 epochs using the conditional generative adversarial network. Each block shows (top) the event-based input representation, (middle) the generated reconstruction, and (bottom) the target frame. The examples illustrate the model’s ability to reconstruct facial structure and expression cues from sparse event patterns.

6.2. Proposed face expression recognition method evaluation

We now assess the proposed framework, evTransFER, using the CK+ and NEFER datasets. Tables 6 and 7 present the consolidated results for the four TIE variants, both with and without LSTM in evTransFER. Both tables indicate that LSTM generally performs best for most variants in the CK+ dataset. Table 6 further reveals that the $f_{\hat{\tau}_k} \cdot h_{\tau_k}$ variant is the most effective for CK+, whereas for NEFER, the variants $f_{\tau_k} \cdot h_{\tau_k}$

and $f_{\hat{\tau}_k} \cdot h_{\hat{\tau}_k}$ yield very similar results. Given that $f_{\hat{\tau}_k} \cdot h_{\tau_k}$ is the top-performing variant in CK+ and performs well in NEFER with LSTM, we will focus on this variant in subsequent experiments for clarity, unless otherwise specified.

Table 6: Performance of the proposed event-based facial expression recognition framework evTransFER on the **e-CK+** dataset, CNN (U-Net) **without** and **with LSTM**, varying the temporal domain measurement and kernel function. The best results for each variant are shown in bold letters.

Encoder (Feat. Ext.)	Top-1 Accuracy			
	$f_{\tau_k} \cdot h_{\tau_k}$	$f_{\tau_k} \cdot h_{\hat{\tau}_k}$	$f_{\hat{\tau}_k} \cdot h_{\tau_k}$	$f_{\hat{\tau}_k} \cdot h_{\hat{\tau}_k}$
evTransFER without LSTM	91,9%	90,5%	92,4%	92,0%
evTransFER with LSTM	93,0%	89,2%	93,6%	93,1%

Table 7: Performance of the proposed event-based facial expression recognition framework evTransFER on the **NEFER** dataset, CNN (U-Net) **without** and **with LSTM**, varying the temporal domain measurement and kernel function. The best results for each variant are shown in bold letters.

Encoder (Feat. Ext.)	Top-1 Accuracy			
	$f_{\tau_k} \cdot h_{\tau_k}$	$f_{\tau_k} \cdot h_{\hat{\tau}_k}$	$f_{\hat{\tau}_k} \cdot h_{\tau_k}$	$f_{\hat{\tau}_k} \cdot h_{\hat{\tau}_k}$
evTransFER without LSTM	70,2%	76,5%	72,0%	76,7%
evTransFER with LSTM	71,4%	76,0%	75,5%	75,9%

6.3. Comparison with State-of-the-Art on the CK+ dataset

Using the e-CK+ database and the setup described in Section 5, in this section, we compare evTransFER with state-of-the-art networks for similar problems, for which the source code is publicly available. In this analysis, we included EST and Asynet, along with a Vision Transformer (ViT) baseline.

For EST, we use the original pipeline described by the authors in [6], with the voxel grid without normalization as input to a classification model, employing a ResNet-34 backbone with a pre-trained encoder fine-tuned for object classification. We also test the case in which three LSTM units are added after the backbone (with the encoder fixed) for EST, and before a fully connected layer. For Asynet, two methods described by the authors in [35] are evaluated: SSR + CNN, where a traditional CNN is used for the sparse representation, and SSR + SCC, where a Submanifold Sparse Convolutional network is used, at a lower computational cost and better model performance. In both cases, the pipeline involves fine-tuning a pre-trained encoder for object classification, with VGG-13 as the backbone. For the ViT [60] we use the vit_b_16 model available in TorchVision. The training parameters for Asynet, EST, and ViT are given in Table 3.

Table 8: Performance on the **e-CK+ dataset** of state-of-the-art methods (SSR & EST) and the here proposed method in facial expression recognition. All methods were trained and evaluated in this database. Asynet, EST, and ViT were trained using the original implementation (FT: fine-tuned). In evTransFER, the U-Net encoder is trained for face reconstruction (FR) and then transferred and fine-tuned to the proposed architecture. The best results with and without LSTM are shown in bold letters.

Method / Reference	Architecture			Encoder training	Top-1 accuracy (%)	Time window (ms)
	Event Data	Encoder (Feat. Ext.)	Sequence learning			
Asynet CNN / [35]	SSR	VGG-16	-	FT	67,2	33,3
Asynet SSC / [35]	SSR	VGG-16	-	FT	67,5	33,3
EST+CNN / [6]	EST	ResNet-34	-	FT	70,9	33,3
ViT / [60]	TIE	vit_b_16	-	FT	79.0	33,3
evTransFER (ours)	TIE	U-Net	-	FR & FT	92,4	33,3
EST+CNN / [6]	EST	ResNet-34	LSTM	FT	83,5	3 x 33,3
ViT / [60]	TIE	vit_b_16	LSTM	FT	78.9	3 x 33,3
evTransFER (ours)	TIE	U-Net	LSTM	FR & FT	93,6	3 x 33,3

Table 8 shows that our proposed method performs much better in the event-based facial expression recognition task (93,6% of accuracy, with LSTM), over state-of-the-art methods. This corresponds to achieving 26.1% points over SSR+SSC, 22.7% points over the original EST (without LSTM), and 10.1% over EST with LSTM.

In summary, the best results on the e-CK+ dataset are achieved using the proposed method evTransFER

6.4. Ablation Study

To assess the significance of the proposed transfer learning methodology for training the U-Net Encoder in evTransFER, we compare three learning approaches:

- **training from scratch**, which involves no prior knowledge from facial frame reconstruction;
- **proposed transfer learning without fine-tuning**, where the encoder is used with fixed weights from the facial frame reconstruction system; and
- **proposed transfer learning with fine-tuning**, which involves using the facial frame reconstruction system and subsequently fine-tuning the encoder’s weights.

. In all three approaches, we evaluate scenarios both with and without LSTM and consider the four TIE variants to clearly demonstrate the impact of the proposed transfer learning approach.

Table 9 presents the results for the proposed method variants with and without LSTM on the e-CK+ dataset. The training approach for the encoder influences the accuracy of the facial expression classifier (Table 9). Training from scratch, without prior knowledge of event-based facial analysis components, yields average performance (76.7% in $f_{\tau_k} \cdot h_{\tau_k}$ without LSTM; and 80.6% in $f_{\hat{\tau}_k} \cdot h_{\hat{\tau}_k}$ with LSTM). Using the reconstruction generator network encoder weights as a static feature extractor improves accuracy by approximately 10% (86.6% in $f_{\tau_k} \cdot h_{\tau_k}$ without LSTM; and 88.7% in $f_{\hat{\tau}_k} \cdot h_{\hat{\tau}_k}$ with LSTM). When fine-tuning by retraining all network weights, including the transferred encoder trained for face reconstruction, the model achieves higher accuracy (92.4% in $f_{\tau_k} \cdot h_{\tau_k}$ without LSTM; and 93.6% in $f_{\hat{\tau}_k} \cdot h_{\hat{\tau}_k}$ with LSTM) compared to the other scenarios.

Table 9: Performance of the proposed event-based facial expression recognition framework evTransFER on the e-CK+ database, varying the temporal domain, measurement function, and kernel function, and **applying different encoder training techniques**. The best results for each variant are shown in bold letters.

Encoder (Feat. Ext.)	Encoder training	Top-1 Accuracy without LSTM (e-CK+)			
		$f_{\tau_k} \cdot h_{\tau_k}$	$f_{\hat{\tau}_k} \cdot h_{\hat{\tau}_k}$	$f_{\tau_k} \cdot h_{\hat{\tau}_k}$	$f_{\hat{\tau}_k} \cdot h_{\tau_k}$
evTransFER: CNN (U-Net)	trained from scratch	72.5%	73.9%	71.8%	76.4%
evTransFER: CNN (U-Net)	transferred	83,1%	85,8%	86,6%	85,7%
evTransFER: CNN (U-Net)	transferred & fine-tuned	91,9%	90,5%	92,4%	92,0%

Encoder (Feat. Ext.)	Encoder training	Top-1 Accuracy with LSTM (e-CK+)			
		$f_{\tau_k} \cdot h_{\tau_k}$	$f_{\hat{\tau}_k} \cdot h_{\hat{\tau}_k}$	$f_{\tau_k} \cdot h_{\hat{\tau}_k}$	$f_{\hat{\tau}_k} \cdot h_{\tau_k}$
evTransFER: CNN (U-Net)	trained from scratch	70.2%	76.9%	74.3%	80.6%
evTransFER: CNN (U-Net)	transferred	86,9%	88,3%	88,7%	88,2%
evTransFER: CNN (U-Net)	transferred & fine-tuned	93,0%	89,2%	93,6%	93,1%

Table 10: Performance of the proposed event-based facial expression recognition framework evTransFER on the NEFER database, varying the temporal domain, measurement function, and kernel function, and **applying different encoder training techniques**. The best results for each variant are shown in bold letters.

Encoder (Feat. Ext.)	Encoder training	Top-1 Accuracy without LSTM (NEFER)			
		$f_{\tau_k} \cdot h_{\tau_k}$	$f_{\hat{\tau}_k} \cdot h_{\hat{\tau}_k}$	$f_{\tau_k} \cdot h_{\hat{\tau}_k}$	$f_{\hat{\tau}_k} \cdot h_{\tau_k}$
evTransFER: CNN (U-Net)	trained from scratch	43,9%	45,5%	47,3%	48,8%
evTransFER: CNN (U-Net)	transferred	70,6%	73,8%	71,5%	67,2%
evTransFER: CNN (U-Net)	transferred & fine-tuned	70,2%	76,5%	72,0%	76,7%

Encoder (Feat. Ext.)	Encoder training	Top-1 Accuracy with LSTM (NEFER)			
		$f_{\tau_k} \cdot h_{\tau_k}$	$f_{\hat{\tau}_k} \cdot h_{\hat{\tau}_k}$	$f_{\tau_k} \cdot h_{\hat{\tau}_k}$	$f_{\hat{\tau}_k} \cdot h_{\tau_k}$
evTransFER: CNN (U-Net)	trained from scratch	43,3%	47,1%	45,0%	49,7%
evTransFER: CNN (U-Net)	transferred	64,0%	72,0%	70,3%	74,1%
evTransFER: CNN (U-Net)	transferred & fine-tuned	71,4%	76,0%	75,5%	75,9%

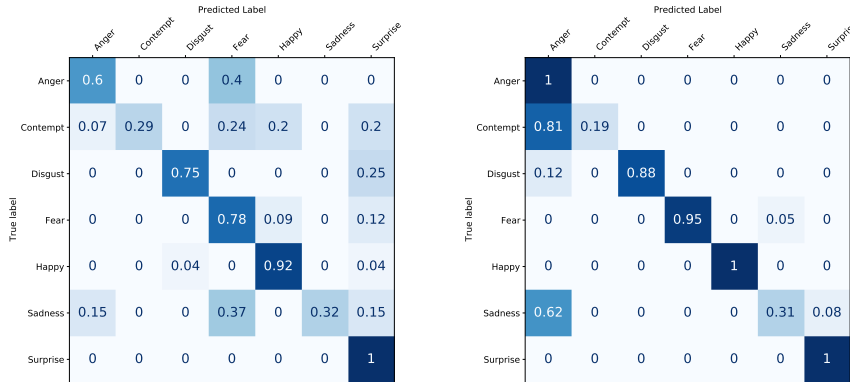
A complementary ablation analysis was conducted on the NEFER dataset (Ta-

ble 10). For real event data, accuracy values are lower than on the e-CK+ dataset due to increased variability, sparser events, and sensor noise in NEFER recordings. The performance patterns remain consistent across datasets. Training the encoder from scratch yields limited recognition performance (43% to 49%, depending on TIE representation and LSTM use), confirming that learning event-based facial representations directly from NEFER is challenging when samples show low event density. Using the reconstruction-trained encoder as a fixed feature extractor improves performance to 73.8% without LSTM and 74.1% with LSTM - a gain of over 25 percentage points compared to training from scratch. This underscores the importance of transferring facial structure priors learned during reconstruction. With fine-tuning, additional gains occur, especially for the $f_{\tau_k} \cdot h_{\hat{\tau}_k}$ and $f_{\hat{\tau}_k} \cdot h_{\tau_k}$ variants. The results of 76.7% (without LSTM) and 76.0% (with LSTM) confirm that adapting the pretrained encoder to NEFER events provides benefits. Unlike in e-CK+, the NEFER dataset shows that LSTM does not always improve performance.

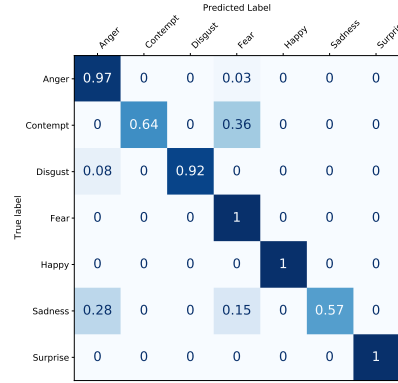
To better illustrate the effect of each training procedure and the use of LSTM, the analysis is complemented by the confusion matrices presented in Figure 9, where we report the best results achieved by the TIE representation ($f_{\tau_k} \cdot h_{\tau_k}$) on the CK+ dataset. As can be observed, the TIE + CNN (ResNet-34) model trained from scratch shows inconsistent results across the different classes (Figure 9 (a)), especially with false positives and negatives in the "Fear" and "Anger" classes, low accuracy for the classes Contempt and Sadness, while classes such as "Happy" and "Surprise" show good results.

6.5. Training and Processing times

We used an NVIDIA DGX-1, a purpose-built system optimized for deep learning. The specifications are presented in Table 11, where up to 2 GPU cores were used for event-based database generation (1 week for e-CK+), event-based encoder training via face reconstruction proxy (≈ 10 hours of training, with 100 epochs), and the application of the classifier training techniques (a few days).



(a) evTransFER: TIE + CNN (U-Net): Encoder trained from scratch - $f_{\tau_k} \cdot h_{\tau_k}$. Accuracy: 76.4% (b) evTransFER: TIE + CNN (U-Net): Encoder transferred from FR - $f_{\tau_k} \cdot h_{\tau_k}$. Accuracy: 86.7%



(c) evTransFER: TIE + CNN (U-Net): Encoder transferred from FR and fine-tuned - $f_{\tau_k} \cdot h_{\tau_k}$. Accuracy: 92.4%

Figure 9: Confusion Matrices of the proposed event-based facial expression recognition framework evTransFER ($f_{\tau_k} \cdot h_{\tau_k}$) and ablations. Left: without LSTM. Right: with LSTM. Top: Encoder Trained from scratch. Center: Encoder Trained for Face Recognition. Bottom: Encoder Trained for Face Recognition and then fine-tuned.

Table 11: Hardware specifications used for experiments and tests in event-based facial expression recognition.

Hardware	Accelerator	Boost clock	Memory Clock	Bandwidth	VRAM	GPU
NVIDIA DGX-1	V100	1530 MHz	1.75Gbit/s	900GB/sec	32GB	GV100

Regarding the inference computation times, we used an NVIDIA GeForce GTX 1050 4GB, with the results for the different methods listed in Table 12. We observe that the proposed method, evTransFER, takes only 3.7 ms (1.6 ms more than EST without LSTM), and when combined with an LSTM, it takes a time comparable to

Asynet. Thus, there is a trade-off: incorporating LSTM temporal models with better results implies a larger sample time window, in this particular case, from 33.3 ms (in the architecture without LSTM) to 3x33 ms (in the architecture with LSTM), which increases processing time and has high latency, but still allows the system to run at the equivalent of 33fps (due to the event-windows size) and with a latency of approximately 25ms.

Table 12: Inference times for event-based facial expression recognition methods.

EST (without LSTM)	Asynet	evTransFER (without LSTM)	evTransFER (with LSTM)
2,09 [ms]	23,4 [ms]	3,71 [ms]	24,69 [ms]

7. Discussion

7.1. Indirect Comparison on various Datasets

Table 13 summarizes performance reported in recent literature using datasets other than e-CK+ employed here. Although a direct comparison between these results and evTransFER is not feasible because of dataset differences and preprocessing, our proposal evTransFER (TIE + CNN trained for FR and fine-tuned + LSTM) outperforms existing methods with 93.6% accuracy. We use the e-CK+ dataset with 346x260 spatial resolution. Two studies report results using similar datasets: ANN+ResNet-18 [34] achieves 92.0% on DVS-CK+ (200x200 pixels), and EST+CNN+LSTM [15] reports 89.1% on e-CK+ (640x480 pixels). [34] preprocesses faces by aligning and cropping them to enhance performance, whereas [15] shows that higher-resolution sensors improve outcomes (results shown at 640x480 for face expression recognition with sequence learning). We use reduced resolution of 346x260 for e-CK+ compared to [15], without adjusting images through face alignment or cropping as in [34].

7.2. TIE representation and Long-term modeling

The experimental analysis highlights the importance of event-based representation and training techniques. The measurement function in TIE plays a crucial role, often

Table 13: Reported performance of state-of-the-art methods on the DVS-CK+, DVS-ADFES, DVS-CASIA, DVS-MMI, NEFER, e-CK+ and e-MMI datasets. The methods use datasets with different spatial resolutions. FR: face reconstruction; FT: fine-tuning.

Database / Reference	Method	Event Data	Encoder training	Top-1 accuracy	Time window	Sensor Spatial Resolution
DVS-CK+ / [34]	ANN	Frames	From Scratch	92,0%	6 x 33ms	200x200
DVS-CK+ / [34]	SNN	Tensor	From Scratch	89,3%	6 x 33ms	200x200
DVS-ADFES / [34]	ANN	Frames	From Scratch	79,6%	6 x 33ms	200x200
DVS-ADFES / [34]	SNN	Tensor	From Scratch	74,2%	6 x 33ms	200x200
DVS-CASIA / [34]	ANN	Frames	From Scratch	72,4%	6 x 33ms	200x200
DVS-CASIA / [34]	SNN	Tensor	From Scratch	69,7%	6 x 33ms	200x200
DVS-MMI / [34]	ANN	Frames	From Scratch	62,0%	6 x 33ms	200x200
DVS-MMI / [34]	SNN	Tensor	From Scratch	63,1%	6 x 33ms	200x200
NEFER / [16]	CNN	TBR [8]	From Scratch	31,0%	15ms	1280x720
NEFER / evTransFER	CNN+LSTM	TIE	FR & FT	76,7%	3 x 33ms	1280x720
e-CK+ / [15]	CNN+LSTM	EST [6]	From Scratch	89,1%	3 x 33ms	640x480
e-MMI / [15]	CNN+LSTM	EST [6]	From Scratch	83,7%	3 x 33ms	640x480
e-CK+ / evTransFER	CNN+LSTM	TIE	FR & FT	93,6%	3 x 33ms	346x260

surpassing the kernel in classifier performance. The findings emphasize the importance of selecting appropriate event representations, effective network architectures, and suitable training techniques for event-based facial expression recognition.

We demonstrate that incorporating LSTM memory units allows evTransFER to sequentially learn from longer-term information on CK+, although no improvement is observed in NEFER. Adding LSTM units requires more processing time but enhances accuracy. Using a 33ms event window (without an LSTM) enables recognition at 33 fps with a processing time of 3.71ms, introducing minimal latency. The systems could be used in real-time. With an LSTM, the latency is 24.69ms, yet the system operates at 33 fps by considering the current 33ms window and two previous ones. This latency could be reduced by reusing the TIE representation and Feature Extraction from previous windows.

7.3. Reconstruction as a Proxy for Encoder Training

A transfer-learning technique enhances framework performance by leveraging a U-Net-based encoder trained for face reconstruction from event sequences. This learning approach requires, during training, only events and corresponding images of the same face, without additional annotations. The reconstruction weights are fine-tuned within the classification system, improving recognition accuracy by 21.5 percentage points, from 72.1% to 92.4% on CK+. We believe this improvement stems from the U-Net’s ability to learn spatio-temporal dynamics in facial expressions, which are crucial for facial expression recognition.

Prior knowledge from facial frame reconstruction significantly enhances model accuracy, as shown in the confusion matrices. When trained from scratch, the encoder’s performance on two of the face expression classes is poor, with an accuracy of approximately 30%. However, training the encoder for recognition and fine-tuning leads to improvements across classes, with the lowest-performing classes reaching 60% and 72% accuracy, and others exceeding 93%. Supervision during encoder reconstruction training helps to understand the spatio-temporal dynamics of facial expressions. This, combined with fine-tuned supervision and an LSTM, effectively captures the structure of facial expression recognition.

We emphasize employing reconstruction as a proxy for training the encoder as a feature extractor in event-based cameras. To understand this, it is important to recognize that event-based datasets remain limited, with fewer real-world datasets containing annotated data. Currently, systems can generate datasets from videos and simulators. Additionally, cameras like DAVIS from iniVation capture event sequences with corresponding frames. By training the encoder through reconstruction as a proxy, along with existing data systems, we can develop encoders without dataset annotations. The image frame to be reconstructed serves as the desired outcome and is required only during training. This strategy could be applied to construct encoders for other object classification problems.

8. Conclusions

This paper introduces a novel learning and classification framework for event-based facial expression recognition, termed evTransFER. This framework features TIE, a representation that effectively normalizes the temporal variable within the structure’s measurement function, enabling a more precise characterization of the spatio-temporal distribution of events. Additionally, it incorporates LSTM to capture long-term dynamics. Furthermore, evTransFER employs a transfer-learning technique utilizing a U-Net-based Encoder, transferred from a facial reconstruction network, significantly enhancing the performance of our recognition framework and offering potential applicability in similar classification contexts.

We assessed the proposed framework using the e-CK+ database. In a state-of-the-art comparative evaluation, evTransFER outperformed other event-based classification models in facial expression recognition. By employing the proposed TIE representation as a latent variable for both reconstruction and classification, the proposed method achieved accuracies of 92.4% without LSTM and 93.6% with LSTM-based temporal learning. Compared to state-of-the-art models, evTransFER significantly outperforms them, achieving 26.1% higher accuracy than SSR+SSC, 22.7% higher than the original EST (without LSTM), and 10.1% higher than EST with LSTM. This enhanced performance is attributed to our event-based facial expression recognition framework, which integrates transfer learning and fine-tuning from facial reconstruction, leveraging prior knowledge and learning the spatio-temporal dynamics of event sequences, as demonstrated in the ablation studies.

In addition to the synthetic e-CK+ dataset, we evaluated evTransFER on NEFER, a real neuromorphic facial expression database. This second evaluation shows that the proposed reconstruction-driven transfer learning strategy substantially improves recognition in real event data, increasing accuracy by more than 25 percentage points compared to training the encoder from scratch. Although the absolute performance on NEFER is naturally lower due to sensor noise, sparsity, and non-uniform event activity, the same patterns observed in e-CK+ are preserved: (i) transfer learning consistently boosts recognition performance, (ii) fine-tuning enables the model to better adapt to the

statistics of real event sequence, and (iii) the temporal domain and kernel configuration $f_{\tau_k} \cdot h_{\hat{\tau}_k}$ remains the most reliable variant. On the other hand, in the NEFER dataset, the use of a LSTM did not improve results.

Future work will explore the use of the learned encoder for other problems (face detection, face recognition, etc.). We also plan to evaluate and adapt the proposed method to classification problems in which the spatio-temporal dynamics of other objects are key, and no annotated data are available; in particular, we will further explore the strategy of building encoders using frame reconstruction as a proxy.

Acknowledgments

This work was partially funded by the FONDEQUIP Project EQM170041.

References

- [1] P. Lichtsteiner, C. Posch, T. Delbruck, A 128×128 120 db 15 μ s latency asynchronous temporal contrast vision sensor, *Solid-State Circuits, IEEE Journal of* 43 (2008) 566 – 576.
- [2] G. Gallego, T. Delbrück, G. Orchard, C. Bartolozzi, B. Taba, A. Censi, S. Leutenegger, A. J. Davison, J. Conradt, K. Daniilidis, D. Scaramuzza, Event-based vision: A survey, *IEEE Transactions on Pattern Analysis and Machine Intelligence* 44 (2022) 154–180.
- [3] X. Zheng, Y. Liu, Y. Lu, T. Hua, T. Pan, W. Zhang, D. Tao, L. Wang, Deep learning for event-based vision: A comprehensive survey and benchmarks, *arXiv preprint arXiv:2302.08890* (2024).
- [4] K. Iddrisu, W. Shariff, P. Corcoran, N. E. O’Connor, J. Lemley, S. Little, Event camera-based eye motion analysis: A survey, *IEEE Access* 12 (2024) 136783–136804.
- [5] B. Chakravarthi, A. A. Verma, K. Daniilidis, C. Fermuller, Y. Yang, Recent event camera innovations: A survey, in: A. Del Bue, C. Canton, J. Pont-Tuset,

- T. Tommasi (Eds.), *Computer Vision – ECCV 2024 Workshops*, Springer Nature Switzerland, Cham, 2025, pp. 342–376.
- [6] D. Gehrig, A. Loquercio, K. Derpanis, D. Scaramuzza, End-to-end learning of representations for asynchronous event-based data, in: *2019 IEEE/CVF International Conference on Computer Vision (ICCV)*, 2019, pp. 5632–5642.
- [7] S. Lin, F. Xu, X. Wang, W. Yang, L. Yu, Efficient spatial-temporal normalization of sae representation for event camera, *IEEE Robotics and Automation Letters* 5 (2020) 4265–4272.
- [8] S. U. Innocenti, F. Becattini, F. Pernici, A. Del Bimbo, Temporal binary representation for event-based action recognition, in: *2020 25th International Conference on Pattern Recognition (ICPR)*, 2021, pp. 10426–10432.
- [9] Y. Dong, T. Zhang, Standard and event cameras fusion for feature tracking, in: *2021 International Conference on Machine Vision and Applications, ICMVA 2021*, Association for Computing Machinery, 2021, p. 55–60.
- [10] A. Mondal, S. R. J. H. Giraldo, T. Bouwmans, A. S. Chowdhury, Moving object detection for event-based vision using graph spectral clustering, in: *2021 IEEE/CVF International Conference on Computer Vision Workshops (ICCVW)*, 2021, pp. 876–884.
- [11] H. Rebecq, R. Ranftl, V. Koltun, D. Scaramuzza, High speed and high dynamic range video with an event camera, *IEEE Transactions on Pattern Analysis and Machine Intelligence* 43 (2021) 1964–1980.
- [12] Y. Zou, Y. Zheng, T. Takatani, Y. Fu, Learning to reconstruct high speed and high dynamic range videos from events, in: *2021 IEEE/CVF Conference on Computer Vision and Pattern Recognition (CVPR)*, 2021, pp. 2024–2033.
- [13] J. Chen, J. Meng, X. Wang, J. Yuan, Dynamic graph cnn for event-camera based gesture recognition, in: *2020 IEEE International Symposium on Circuits and Systems (ISCAS)*, 2020, pp. 1–5.

- [14] J. Kim, J. Bae, G. Park, D. Zhang, Y. M. Kim, N-imagenet: Towards robust, fine-grained object recognition with event cameras, in: Proceedings of the IEEE/CVF International Conference on Computer Vision (ICCV), 2021, pp. 2146–2156.
- [15] R. Verschae, I. Bugueno-Cordova, Event-based gesture and facial expression recognition: A comparative analysis, *IEEE Access* 11 (2023) 121269–121283.
- [16] L. Berlincioni, L. Cultrera, C. Albisani, L. Cresti, A. Leonardo, S. Picchioni, F. Becattini, A. Del Bimbo, Neuromorphic event-based facial expression recognition, in: 2023 IEEE/CVF Conference on Computer Vision and Pattern Recognition Workshops (CVPRW), 2023, pp. 4109–4119.
- [17] W. Zhao, R. Chellappa, P. J. Phillips, A. Rosenfeld, Face recognition: A literature survey, *ACM computing surveys (CSUR)* 35 (2003) 399–458.
- [18] R. Jafri, H. R. Arabnia, A survey of face recognition techniques, *Journal of information processing systems* 5 (2009) 41–68.
- [19] M. Wang, W. Deng, Deep face recognition: A survey, *Neurocomputing* 429 (2021) 215–244.
- [20] F. Becattini, L. Berlincioni, L. Cultrera, A. Del Bimbo, Neuromorphic face analysis: A survey, *Pattern Recognition Letters* 187 (2025) 42–48.
- [21] G. Chen, L. Hong, J. Dong, P. Liu, J. Conradt, A. Knoll, Eddd: Event-based drowsiness driving detection through facial motion analysis with neuromorphic vision sensor, *IEEE Sensors Journal* 20 (2020) 6170–6181.
- [22] T. Kanamaru, T. Arakane, T. Saitoh, Isolated single sound lip-reading using a frame-based camera and event-based camera, *Frontiers in Artificial Intelligence* 5 (2023) 1070964.
- [23] G. Moreira, A. Graça, B. Silva, P. Martins, J. Batista, Neuromorphic event-based face identity recognition, in: 2022 26th International Conference on Pattern Recognition (ICPR), 2022, pp. 922–929.

- [24] F. Becattini, F. Palai, A. D. Bimbo, Understanding human reactions looking at facial microexpressions with an event camera, *IEEE Transactions on Industrial Informatics* 18 (2022) 9112–9121.
- [25] S. Barua, Y. Miyatani, A. Veeraraghavan, Direct face detection and video reconstruction from event cameras, in: *2016 IEEE Winter Conference on Applications of Computer Vision (WACV)*, 2016, pp. 1–9.
- [26] G. Lenz, S.-H. Ieng, R. Benosman, Event-based face detection and tracking using the dynamics of eye blinks, *Frontiers in Neuroscience* 14 (2020).
- [27] B. Ramesh, H. Yang, Boosted kernelized correlation filters for event-based face detection, in: *2020 IEEE Winter Applications of Computer Vision Workshops (WACVW)*, 2020, pp. 155–159.
- [28] U. Bissarinova, T. Rakhimzhanova, D. Kenzhebalin, H. A. Varol, Faces in event streams (fes): An annotated face dataset for event cameras, *Sensors* 24 (2024).
- [29] S. Himmi, V. Parret, A. Chhatkuli, L. V. Gool, Ms-evs: Multispectral event-based vision for deep learning based face detection, in: *2024 IEEE/CVF Winter Conference on Applications of Computer Vision (WACV)*, 2024, pp. 605–614.
- [30] A. N. Angelopoulos, J. N. Martel, A. P. Kohli, J. Conradt, G. Wetzstein, Event-based near-eye gaze tracking beyond 10,000 hz, *IEEE Transactions on Visualization and Computer Graphics* 27 (2021) 2577–2586.
- [31] Y. Wu, H. Han, J. Chen, W. Zhai, Y. Cao, Z.-j. Zha, Brat: Bidirectional relative positional attention transformer for event-based eye tracking, in: *Proceedings of the Computer Vision and Pattern Recognition Conference*, 2025, pp. 5136–5144.
- [32] H. Huang, X. Lin, H. Ren, Y. Zhou, B. Cheng, Exploring temporal dynamics in event-based eye tracker, in: *Proceedings of the Computer Vision and Pattern Recognition Conference*, 2025, pp. 5145–5154.
- [33] H. M. Truong, V.-T. Ly, H. G. Tran, T.-P. Nguyen, T. T. Doan, Dual-path enhancements in event-based eye tracking: Augmented robustness and adaptive temporal

- modeling, in: Proceedings of the Computer Vision and Pattern Recognition Conference, 2025, pp. 5155–5163.
- [34] S. Barchid, B. Allaert, A. Aissaoui, J. Mennesson, C. C. Djeraba, Spiking-fer: Spiking neural network for facial expression recognition with event cameras, in: Proceedings of the 20th International Conference on Content-Based Multimedia Indexing, CBMI '23, Association for Computing Machinery, 2023, p. 1–7.
- [35] N. Messikommer, D. Gehrig, A. Loquercio, D. Scaramuzza, Event-based asynchronous sparse convolutional networks, in: Computer Vision – ECCV 2020, Springer International Publishing, Cham, 2020, pp. 415–431.
- [36] R. W. Baldwin, M. Almatrafi, J. R. Kaufman, V. Asari, K. Hirakawa, Inceptive event time-surfaces for object classification using neuromorphic cameras, in: Image Analysis and Recognition, 2019, pp. 395–403.
- [37] R. Baldwin, R. Liu, M. M. Almatrafi, V. K. Asari, K. Hirakawa, Time-ordered recent event (tore) volumes for event cameras, IEEE Transactions on Pattern Analysis and Machine Intelligence (2022).
- [38] J. Wan, M. Xia, Z. Huang, L. Tian, X. Zheng, V. Chang, Y. Zhu, H. Wang, Event-based pedestrian detection using dynamic vision sensors, Electronics 10 (2021).
- [39] Z. Wang, F. Cladera, A. Bisulco, D. Lee, C. J. Taylor, K. Daniilidis, M. A. Hsieh, D. D. Lee, V. Isler, Ev-catcher: High-speed object catching using low-latency event-based neural networks, IEEE Robotics and Automation Letters 7 (2022) 8737–8744.
- [40] Z. Huang, L. Sun, C. Zhao, S. Li, S. Su, Eventpoint: Self-supervised interest point detection and description for event-based camera, in: 2023 IEEE/CVF Winter Conference on Applications of Computer Vision (WACV), 2023, pp. 5385–5394.
- [41] Y. Bi, A. Chadha, A. Abbas, E. Bourtsoulatze, Y. Andreopoulos, Graph-based spatio-temporal feature learning for neuromorphic vision sensing, IEEE Transactions on Image Processing 29 (2020) 9084–9098.

- [42] G. Orchard, A. Jayawant, G. K. Cohen, N. Thakor, Converting static image datasets to spiking neuromorphic datasets using saccades, *Frontiers in Neuroscience* 9 (2015).
- [43] A. Amir, B. Taba, D. Berg, T. Melano, J. McKinstry, C. Di Nolfo, T. Nayak, A. Andreopoulos, G. Garreau, M. Mendoza, J. Kusnitz, M. Debole, S. Esser, T. Delbruck, M. Flickner, D. Modha, A low power, fully event-based gesture recognition system, in: *2017 IEEE Conference on Computer Vision and Pattern Recognition (CVPR)*, 2017, pp. 7388–7397.
- [44] S. B. Shrestha, G. Orchard, SLAYER: Spike layer error reassignment in time, in: *Advances in Neural Information Processing Systems* 31, 2018, pp. 1419–1428.
- [45] J. Kaiser, A. Friedrich, J. V. Tieck, D. Reichard, A. Roennau, E. Neftci, R. Dillmann, Embodied neuromorphic vision with continuous random backpropagation, in: *2020 8th IEEE RAS/EMBS International Conference for Biomedical Robotics and Biomechatronics (BioRob)*, 2020, pp. 1202–1209.
- [46] J. Kaiser, H. Mostafa, E. Neftci, Synaptic plasticity dynamics for deep continuous local learning (decolle), *Frontiers in Neuroscience* 14 (2020).
- [47] X. Lagorce, G. Orchard, F. Galluppi, B. E. Shi, R. B. Benosman, Hots: A hierarchy of event-based time-surfaces for pattern recognition, *IEEE Transactions on Pattern Analysis and Machine Intelligence* 39 (2017) 1346–1359.
- [48] A. Sironi, M. Brambilla, N. Bourdis, X. Lagorce, R. Benosman, HATS: Histograms of averaged time surfaces for robust event-based object classification, in: *Proceedings of the IEEE Conference on Computer Vision and Pattern Recognition*, openaccess.thecvf.com, 2018, pp. 1731–1740.
- [49] H. Gammulle, S. Denman, S. Sridharan, C. Fookes, Two stream lstm: A deep fusion framework for human action recognition, in: *2017 IEEE Winter Conference on Applications of Computer Vision (WACV)*, 2017, pp. 177–186.

- [50] P. Pansuriya, N. Chokshi, D. Patel, S. Vahora, Human activity recognition with event-based dynamic vision sensor using deep recurrent neural network, *International Journal of Advanced Science and Technology* 29 (2020) 9084–9091.
- [51] C. Ryan, B. O’Sullivan, A. Elrasad, A. Cahill, J. Lemley, P. Kieilty, C. Posch, E. Perot, Real-time face & eye tracking and blink detection using event cameras, *Neural Networks* 141 (2021) 87–97.
- [52] H. Rebecq, D. Gehrig, D. Scaramuzza, Esim: an open event camera simulator, in: *Proceedings of The 2nd Conference on Robot Learning*, volume 87 of *Proceedings of Machine Learning Research*, PMLR, 2018, pp. 969–982.
- [53] Y. Hu, S.-C. Liu, T. Delbruck, v2e: From video frames to realistic dvs events, in: *2021 IEEE/CVF Conference on Computer Vision and Pattern Recognition Workshops (CVPRW)*, 2021, pp. 1312–1321.
- [54] S. Niklaus, L. Mai, F. Liu, Video frame interpolation via adaptive convolution, in: *2017 IEEE Conference on Computer Vision and Pattern Recognition (CVPR)*, 2017, pp. 2270–2279.
- [55] H. Liu, J. Xu, S. Peng, Y. Chang, H. Zhou, Y. Duan, L. Zhu, Y. Tian, L. Yan, NER-Net+: Seeing Motion at Nighttime With an Event Camera , *IEEE Transactions on Pattern Analysis & Machine Intelligence* 47 (2025) 4768–4786.
- [56] P. Isola, J.-Y. Zhu, T. Zhou, A. A. Efros, Image-to-image translation with conditional adversarial networks, in: *2017 IEEE Conference on Computer Vision and Pattern Recognition (CVPR)*, 2017, pp. 5967–5976.
- [57] O. Ronneberger, P. Fischer, T. Brox, U-net: Convolutional networks for biomedical image segmentation, in: *Medical Image Computing and Computer-Assisted Intervention – MICCAI 2015*, 2015, pp. 234–241.
- [58] P. Lucey, J. F. Cohn, T. Kanade, J. M. Saragih, Z. Ambadar, I. Matthews, The extended cohn-kanade dataset (ck+): A complete dataset for action unit and emotion-specified expression, *2010 IEEE Computer Society Conference on Computer Vision and Pattern Recognition - Workshops* (2010) 94–101.

- [59] T. Kanade, Y. li Tian, J. F. Cohn, Comprehensive database for facial expression analysis, Proceedings Fourth IEEE International Conference on Automatic Face and Gesture Recognition (Cat. No. PR00580) (2000) 46–53.
- [60] A. Dosovitskiy, L. Beyer, A. Kolesnikov, D. Weissenborn, X. Zhai, T. Unterthiner, M. Dehghani, M. Minderer, G. Heigold, S. Gelly, et al., An image is worth 16x16 words: Transformers for image recognition at scale, arXiv preprint arXiv:2010.11929 (2020).